Synchronous volcanic eruptions and abrupt climate change ~17.7k years ago plausibly linked by stratospheric ozone depletion

Joseph R. McConnell[1], Andrea Burke[2], Nelia W. Dunbar[3], Peter Köhler[4], Jennie L. Thomas[5], Monica M. Arienzo[1], Nathan J. Chellman[1], Olivia J. Maselli[1], Michael Sigl[1], Jess F. Adkins[6], Daniel Baggenstos[7], John F. Burkhart[8], Edward J. Brook[9], Christo Buizert[9], Jihong Cole-Dai[10], T.J. Fudge[11], Gregor Knorr[4], Hans-F. Graf[12], Mackenzie M. Grieman[13], Nels Iverson[3], Shaun A. Marcott[9,14], Kenneth C. McGwire[1], Robert Mulvaney[15], Guillaume Paris[6], Rachael H. Rhodes[9,12], Eric S. Saltzman[13], Jeffrey P. Severinghaus[7], Jørgen-Peder Steffensen[16], Kendrick C. Taylor[1], Gisela Winckler[17]

[1]Desert Research Institute, Reno, USA
[2]University of St. Andrews, St. Andrews, UK
[3]New Mexico Institute of Mining and Technology, Socorro, USA
[4]Alfred-Wegener-Institut (AWI) Helmholtz-Zentrum für Polar- und Meeresforschung, Bremerhaven, Germany
[5]Université Versailles St-Quentin, Paris, France
[6]California Institute of Technology, Pasadena, USA
[7]Scripps Institute of Oceanography, La Jolla, USA
[8]University of Oslo, Oslo, Norway
[9]Oregon State University, Corvallis, USA
[10]South Dakota State University, Brookings, USA
[11]University of Washington, Seattle, USA
[12]University of Cambridge, Cambridge, UK
[13]University of California, Irvine, USA
[14]University of Wisconsin, Madison, USA
[15]British Antarctic Survey, Cambridge, UK
[16]University of Copenhagen, Copenhagen, DK
[17]Lamont Doherty Earth Observatory, Palisades, USA

Classification
Physical Sciences: Earth, Atmospheric, and Planetary Sciences

Corresponding Author
Joseph R. McConnell, Desert Research Institute, 2215 Raggio Parkway, Reno NV 89512 USA
(Email: Joe.McConnell@dri.edu; Phone: 775-673-7348; Fax: 775-673-7363)

Abstract

Glacial-state greenhouse gas concentrations and Southern Hemisphere climate conditions persisted until approximately 17.7k years ago when a nearly synchronous acceleration in deglaciation was recorded in paleoclimate proxies in large parts of the Southern Hemisphere, with many changes ascribed to a sudden poleward shift in the Southern Hemisphere westerlies and subsequent climate impacts. We used high-resolution chemical measurements in the WAIS Divide, Byrd, and other ice cores to document a unique, ~192-year series of halogen-rich volcanic eruptions exactly at the start of accelerated deglaciation, with tephra identifying the nearby Mt. Takahe volcano as the source. Extensive fallout from these massive eruptions has been found >2800 km from Mt. Takahe. Sulfur isotope anomalies and marked decreases in ice core bromine consistent with increased surface ultraviolet radiation indicate that the eruptions led to stratospheric ozone depletion. Rather than a highly improbable coincidence, circulation and climate changes extending from the Antarctic Peninsula to the subtropics – similar to those associated with modern stratospheric ozone depletion over Antarctica – plausibly link the Mt. Takahe eruptions to the onset of accelerated Southern Hemisphere deglaciation approximately 17.7k years ago.

Significance

Cold and dry glacial-state climate conditions persisted in the Southern Hemisphere until approximately 17.7k years ago when paleoclimate records show a largely unexplained sharp, nearly synchronous acceleration in deglaciation. Detailed measurements in Antarctic ice cores document exactly at that time a unique, ~192-year series of massive halogen-rich volcanic eruptions geochemically attributed to Mt. Takahe in West Antarctica. Rather than a coincidence, we postulate that halogen-catalyzed stratospheric ozone depletion over Antarctica triggered large-scale atmospheric circulation and hydroclimate changes similar to the modern Antarctic ozone hole, explaining the synchronicity and abruptness of accelerated Southern Hemisphere deglaciation.

\body

Long-term variations in global climate, such as the glacial/interglacial cycles recorded in paleo-archives, are linked to changes in Earth's orbital parameters and insolation (1). Superimposed on this smooth, orbital-scale variability are abrupt changes in climate, resulting in substantial variations among glacial terminations (2) and suggesting that the evolution of each deglaciation may be influenced by climate drivers specific to that deglaciation (3). One such rapid change during the last termination began approximately 17.7k years before 1950 (17.7ka) when paleoclimate records show sharp, nearly synchronous changes across the Southern Hemisphere (SH) such as a widespread retreat of glaciers in Patagonia (4, 5) and New Zealand (6), onset of rapid lake expansion in the Bolivian Andes (7), increases in summertime precipitation in subtropical Brazil (8), decreases in southern Australian aridity (9), and dust deposition recorded in ocean sediment cores (Fig. 1) (9, 10). At the same time, Antarctic ice cores record a sharp decrease in SH continental dust (11), a widespread decline in sea salt deposition, a marked upturn in water isotopic ratios indicating warming (12, 13), and a trend of increasing atmospheric methane (CH_4) (12) and carbon dioxide (CO_2) (14, 15) coincident with a drop in the stable carbon isotopic ratios in CO_2 (14) (Fig. 1). Although the causes are not certain, many of these rapid changes have been attributed to a sudden poleward shift in the westerly winds encircling Antarctica – with resulting changes in SH hydroclimate, sea ice extent, ocean circulation (6, 7, 9), and ventilation of the deep Southern Ocean (16).

The new very high-time-resolution WAIS Divide (WD) (12) ice core record from West Antarctica (Materials and Methods) shows that following a long period of relative stability extending glacial-state climate conditions (>10k years after the 65°S annually integrated insolation minimum marking the Last Glacial Maximum [LGM]), sea salt and SH continental dust aerosol concentrations, snowfall rates, water isotope ratios, and greenhouse gas concentrations (CO_2 (15), CH_4) changed at 17.7ka or soon after, sharply at first and then more gradually (Fig. 1). Concentrations of the traditional continental dust tracer non-sea-salt calcium (nssCa) dropped 100-fold from ~7 ng g^{-1} during the LGM to ~0.07 ng g^{-1} during the early Holocene, with nearly 50% of the total decrease occurring during the 400 years after 17.7ka. Sea-salt-sodium concentration (ssNa), thought to be a proxy for sea ice formation, decreased five-fold during the deglaciation with approximately 40% of the decline occurring in this same period (12). About 25% of the ~8‰ $\delta^{18}O$ and 10% of the 320 parts-per-billion CH_4 overall increases from LGM to the early Holocene values happened during these 400 years (12) (Fig. 1).

Measurements of nssCa and other SH dust proxies in the WD core (Figs. 1, 2) (SI Appendix, Fig. S1) – complemented by new measurements in archived samples of the Byrd core (17) located 159 km from WD (Fig. 3) (SI Appendix, Fig. S2) – indicate that the abrupt climate change started in central West Antarctica~17.7k years ago with the sharp and sustained decline in SH continental dust deposition (Fig. 1) nearly synchronous (SI Appendix – Continuous Ice Core Measurements) with the start of marked increases in CH_4 and CO_2 (Fig. 2). Starting ~60 (±18) years prior to the abrupt drop in dust and extending ~132 years after was a unique, long-lived glaciochemical anomaly originally detected in limited discrete measurements of acidity, chloride, and fluoride in the Byrd core (SI Appendix, Fig. S3) (17). New continuous measurements of a broad range of elements and chemical species in the WD and Byrd cores (SI Appendix, Figs. S1, S2) show that the glaciochemical anomaly consisted of nine pulses measured between 2426.97 to 2420.04 m depth in the WD core, corresponding to a ~192-year period from 17.748 to 17.556 ka (Fig. 2) on the WD2014 timescale (18). Evidence of this glaciochemical anomaly also has been traced throughout West Antarctica and parts of East Antarctica in ice cores (17) (Figs. 3) (SI Appendix, Fig. S3) and radar surveys (19).

Mt. Takahe 17.7ka Volcanic Event

Elements and chemical species associated with seawater (e.g., sodium, magnesium, calcium, strontium), fallout from biomass burning (e.g., black carbon, ammonium, nitrate), and continental dust (e.g., aluminum, calcium, vanadium, iron, rubidium, barium) showed little or no change during the glaciochemical anomaly in both the WD (Fig. 2) and Byrd cores (SI Appendix, Figs. S1, S2). Other elements increased by up to fifty times background concentrations, however, including rare earth elements (REE) that normally are associated with insoluble particles and low-boiling-point heavy metals linked in past studies to Antarctic volcanic emissions (20). Concentration changes differed between elements (SI Appendix, Figs. S1, S2), with increases above background levels during nine distinct pulses of 1.7-fold for sulfur; up to six-fold for chlorine; 10-fold for lead; 20-fold for cerium, lanthanum, and thallium; and 50-fold for bismuth. While no increases were observed in the smaller (0.8 to 2.4 micron) insoluble particle size fraction, 2.5- and 11-fold increases were found for the medium (2.4 to 4.5 micron) and larger (4.5 to 9.5 micron) fractions, respectively (SI Appendix, Fig. S1). Of all our ~35 chemical measurements, only bromine and bromide concentrations (SI Appendix – Bromine and Bromide) declined during this ~192-year period (Fig. 1) (SI Appendix, Figs. S1, S2).

Consistent with the initial interpretation of the original Byrd measurements (17) but in contrast to subsequent interpretations (21) (Materials and Methods), the very pronounced enrichments of low-boiling-point heavy metals (20) and halogens (22), as well as elevated concentrations of medium and larger insoluble particle fractions in the WD core (Fig. 2) (SI Appendix, Fig. S1) clearly indicate a volcanic source for the glaciochemical anomaly (23). Although sulfur during the anomaly was relatively low (Fig. 4), the S/Cl mass ratio was ~0.1 which is nearly identical to the 0.095 ratio reported for modern emissions from nearby Mt. Erebus (23). Moreover, tephra particles from the anomaly (Materials and Methods) analyzed by electron microprobe showed mineralogy of a trachytic volcanic eruption (SI Appendix, Table S1) geochemically consistent with tephra from nearby Mt. Takahe (24, 25) (76.28°S, 112.08°W) – a recently active, flat-topped stratovolcano in West Antarctica located 360 km north of the WD coring site (Fig. 3). Therefore, we refer to the ~192-year series of volcanic eruptions as the "17.7ka Mt. Takahe Event." Estimates of emissions from Mt. Takahe from enhancements in chlorine fluxes measured in the WD, Byrd, and Taylor Glacier cores, as well as radar-based evidence on the extent of the fallout plume (Fig. 3), suggest that average and peak chlorine emissions were ~100 and ~400 Gg y^{-1}, respectively (SI Appendix – Mt. Takahe Emissions Estimates). These levels are ~10 and ~40 times higher than modern emissions estimated for Mt. Erebus (23), as well as ~0.4 and ~1.6 times those reported for Mt. Etna, currently the largest point source of chlorine on Earth (22). We estimate that transport of only 1% of the 17.7ka Mt. Takahe emissions to the high-latitude SH stratosphere would have yielded chlorine concentrations comparable to those responsible for modern chlorofluorocarbon-driven ozone depletion.

All of our measurements in the WD, Byrd, and Taylor Glacier (Materials and Methods) cores clearly indicate that the 17.7ka event resulted from a series of massive halogen-rich, volcanic eruptions in West Antarctica (Figs. 1, 2) (SI Appendix, Figs. S1-S3). Explosive volcanic eruptions inject large amounts of sulfur and other aerosols often including halogens into the stratosphere, frequently leading to stratospheric ozone depletion even for small eruptions (26-28) and an increase in UV radiation at Earth's surface. Photolysis and precipitation scavenging at warmer, lower-latitude sites limit atmospheric lifetimes of volcanic halogens and so impacts on stratospheric ozone, although transport of even a small fraction of halogen emissions to the stratosphere can deplete ozone (29). Halogen lifetimes during the 17.7ka event, however, were extended at Mt. Takahe by the extremely cold and dry LGM conditions, particularly during dark winter months. Such a massive and persistent (~192 year) series of halogen-rich volcanic eruptions is unique within the ~68k-year WD ice core record, and the event straddles the most significant abrupt climate change recorded in Antarctic ice cores and other SH climate proxies during the >10k-year period of the last deglaciation (Figs. 1, 2) which occurred many thousands of years after the 65°S LGM insolation minimum. The probability that these two unique events coincided by chance is the product of the two individual probabilities and on the order of one in a million. Rather than a highly improbable coincidence, we hypothesize that these massive halogen-rich eruptions are linked causally by stratospheric ozone depletion to large-scale changes in SH climate and related changes in atmospheric and oceanic circulation analogous to those from modern, halogen-catalyzed ozone depletion.

Evidence for Stratospheric Ozone Depletion

Evidence for ejection of volcanic material from the 17.7ka Mt. Takahe Event into the stratosphere and/or enhanced tropospheric ultraviolet (UV) radiation was found in sulfur isotope anomalies in the WD and Byrd cores (Fig. 4). Sulfur concentrations during the ~192-year event were 1.7 times higher than background and $\delta^{34}S$ values were lower, indicating a volcanic source of the elevated sulfur since background marine and volcanic sources have $\delta^{34}S$ signatures of 15 to 21‰ and 0 to 5‰, respectively (30). Furthermore, exposure to UV radiation, such as when volcanic sulfur is ejected into the stratosphere above the ozone layer, generates distinct changes in sulfur isotope mass independent fractionation (MIF; expressed as non-zero values of $\Delta^{33}S$). Previous studies have shown that MIF from a single eruption into the stratosphere follows a distinct evolution from positive to negative $\Delta^{33}S$ during the course of sulfate deposition (31), so low-resolution sampling and multiple overlapping explosive events may result in small values of $\Delta^{33}S$ even for stratospheric eruptions. The $\Delta^{33}S$ of sulfate from prior to the 17.7ka event was within 2σ uncertainty of zero as expected for non-stratospheric sulfate (31, 32). The non-zero $\Delta^{33}S$ measured in the ice during the 17.7ka event indicated that the volcanic sulfur was indeed bombarded by enhanced UV radiation, either in the stratosphere as a result of ejection above the ozone layer and/or in the troposphere after significant stratospheric ozone depletion. The resolution of the WD and Byrd samples, the multiple explosive phases of the Mt. Takahe eruptions, and the low concentration of volcanic sulfur above background levels, however, meant that the magnitude of the MIF anomaly was significant outside of 2σ only for a few samples (Materials and Methods).

Evidence for stratospheric ozone depletion and enhanced near-surface UV radiation also comes from changes in bromine concentration in the WD and Byrd ice core records. Photochemical reactions in near-surface snow cause rapid cycling between the snow and air for a broad range of reactive and volatile chemical species including bromine and nitrate, and a net loss in the snow through time known as reversible deposition (33, 34). The magnitude of this loss primarily depends on the duration and intensity of exposure of the snow to UV radiation, with duration determined by the burial rate (SI Appendix – Evidence for Reversible Bromine Deposition in Antarctic Snow) since light penetration below ~0.3 m in the snowpack is much reduced and exposure intensity is determined by the level of impinging UV radiation. During 27ka to 6ka in the WD record, there were only two sustained declines in bromine concentration; and the longest and most pronounced decline exactly coincided with the 17.7ka Mt. Takahe Event (Fig. 1). Annual layering in fine insoluble dust particle concentrations in the WD record indicates that the snowfall rate did not change during this period, eliminating burial rate variations as the cause of the bromine decline and implicating increased surface UV radiation (SI Appendix – Snowpack Modeling).

While bromine release from the snowpack is sensitive to changes in UV radiation and that sensitivity increases with snow acidity (33), photochemical model simulations as well as examination of the WD record show that acidity alone is not sufficient to explain the observed bromine depletion. First, bromine concentrations in the WD and Byrd cores remained low even during periods between the nine volcanic pulses of the 17.7ka Mt. Takahe Event when concentrations of nearly all elements and chemical species including acidity returned to near background concentrations (SI Appendix, Figs. S1, S2). WD snow accumulation was relatively high (>100 kg m^{-2} y^{-1}) during this period (35) so the regions of high acidity in the core were well separated from regions of low acidity. Second, consistent with modern observations in which some but not all volcanic eruptions are associated with ozone depletion (26), evaluation of the

100 highest acidity events (annual average concentration >3.0 μeq L^{-1}) in the 10ka to 25ka WD record show that 30% were not associated with bromine depletion and that depletion was not proportional to acidity (SI Appendix, Fig. S6). This clearly demonstrates that acidity alone did not lead to bromine depletion and suggests that both increased acidity and increased UV radiation were required as predicted by modeling (SI Appendix – Snowpack Modeling).

It is unclear whether modern ozone depletion and enhanced surface UV have resulted in bromine depletion in near-surface snow. First, modern chlorofluorocarbon-driven ozone depletion largely has been confined to spring while volcanically driven Mt. Takehe ozone depletion may have persisted throughout the austral summer when the impact on snowpack photochemistry was greater. Second, there was no recent increase in acidity in Antarctic snow so the sensitivity of bromine re-emission to enhanced UV radiation was low. Third, no suitable Antarctic ice core record of bromine was available to assess the modern period (SI Appendix – Comparisons to Modern Ozone Depletion).

Plausible Linkages to Rapid SH Deglaciation

Observations and climate model simulations indicate that modern anthropogenic ozone depletion is linked to surface climate changes throughout the SH substantially similar to those approximately 17.7ka ago, as documented in paleoclimate archives. These include a poleward shift and acceleration of the westerly winds around Antarctica (36), acceleration of mid-latitude easterly winds (36), and southward expansion of the summertime Hadley cell – leading to changes in temperature and precipitation extending from the Antarctic Peninsula (37) to the subtropics especially during austral summer (38). Specific climate changes include subtropical moistening and mid-latitude drying (Fig. 5) (38), as well as pronounced warming in the northern Antarctic Peninsula and Patagonia, with cooling over the Antarctic continent, particularly in East Antarctica (36). Enhanced deep-ocean ventilation around Antarctica with reduction in oceanic uptake of CO_2 (39), also is associated with these modern changes in the westerlies. Quasi-equilibrium simulations of the potential impacts of a sustained ozone hole at 17.7ka using a coupled Atmosphere Ocean General Circulation Model (AOGCM) initialized to LGM conditions predict qualitatively similar responses compared to the modern ozone hole. These results include surface warming of 0.4 to 0.8°C over all of Antarctica and the Southern Ocean, in agreement with quasi-equilibrium simulations of the modern ozone hole (40, 41) (SI Appendix – AOGCM Simulations). These longer-term surface temperature responses are separate from the initial cooling simulated for modern stratospheric ozone depletion (42).

Previous studies (e.g., (43)) suggested that rising insolation initiated melting of Northern Hemisphere (NH) ice sheets at 19 ka, which triggered a reduction in the strength of the Atlantic overturning circulation, and through the bi-polar seesaw resulted in SH warming and CO_2 release from the Southern Ocean, although the exact mechanisms driving the CO_2 release are still debated. We postulate that the ~192-year series of halogen-rich eruptions of Mt. Takahe and the subsequent ozone hole (26) initiated a series of events analogous to the modern ozone hole that acted to accelerate deglaciation at 17.7ka. First, stratospheric ozone depletion changed SH atmospheric circulation resulting in a rapid increase and poleward shift in the westerlies (36) (SI Appendix, Fig. S7). Second, consequent widespread perturbations in SH hydrometeorology, including increased austral summer subtropical precipitation between ~15^{o} and ~35^{o}S (Figs. 1f, 5), led to enhanced CH_4 wetland emissions (44). Third, in combination with subtropical increases, decreased mid-latitude precipitation, and lower wind speeds between ~35^{o} and ~50^{o}S (Fig. 5) (8, 38, 45), as well as warming centered at ~60^{o}S (36) (SI Appendix, Fig. S7), altered climate throughout SH LGM dust source regions (46), causing a pronounced, synchronous, ~50% decline in SH dust deposition (Fig. 1), reducing ocean biological uptake (10, 47) and thereby sharply reducing the ocean CO_2 sink. In Patagonia and New Zealand, warmer and dryer conditions south of ~35°S (38) led to the well-documented retreat of glaciers (4-6) that starved glacial outwash plains of their fine sediment resupply (46), with lower wind speeds possibly also contributing to reduced dustiness (48). In aridity-driven SH dust source regions located north of ~35°S (Australia, Africa, extratropical South America), a cooler and wetter climate (38) sharply reduced aridity and hence dust export (9). Fourth, westerlies shifted poleward (SI Appendix, Fig. S8) and thus altered sea-ice extent leading to changes in upwelling of deep ocean carbon and nutrients particularly in austral summer when, because of minimal sea ice and generally lower wind speeds, impacts on the carbon cycle were most pronounced (49). The net effect of these physical and biological pumps on the carbon cycle (16) likely started the release of CO_2 and initiated the rise in atmospheric CO_2 that followed the 17.7ka Mt. Takahe Event (Fig. 1) (14, 15). As with modern increases in greenhouse gases (50), the atmospheric and oceanic circulation as well as hydroclimatic changes initiated by stratospheric ozone depletion were reinforced by rising CO_2 (15) and CH_4 (12, 16) .

Conclusion

Although the climate system already was primed for the switch from a glacial to interglacial state by insolation changes (1) and NH land ice loss (43), the ~192-year ozone hole resulting from the halogen-rich eruptions of Mt. Takahe plausibly provided supplementary forcing during the last termination that drove the westerly wind belt poleward and altered SH hydroclimate, providing a straightforward explanation for the synchronicity and abruptness of the SH climatic changes and global greenhouse gases that occurred approximately 17.7k years ago.

Materials and Methods

Ice Core Measurements. A nearly contiguous set of longitudinal WD samples from 1300 m to 2710 m depth was analyzed using a state-of-the-art continuous ice core analytical system (51-54) (SI Appendix, Fig. S8), in addition to replicate WD samples from 2419.3 m to 2435.2 m and all samples of the Byrd core (17) available from the University of Copenhagen archive between 1242.06 to 1303.39 m depth (SI Appendix – Continuous Ice Core Measurements). Samples from Taylor Glacier in the Antarctic Dry Valleys (55) also provided a record of the Mt. Takahe event (Fig. 3). Additional measurements including fluoride, bromide, and methane sulfonic acid (MSA) were made on discrete samples (SI Appendix – Discrete Ice Core Measurements).

Sulfur isotopes were measured on selected discrete samples using multi-collector ICP-MS (56). The measured isotopic ratios were converted to δ values (VCDT) using the IAEA standards S5 and S6 and the standard NBS127. The $\delta^{34}S$ and $\delta^{33}S$ values of $NaSO_4$ ($\Delta^{33}S = 0$) were used to calibrate the instrument. The instrumental uncertainty for $\Delta^{33}S$, defined as two times the standard deviation (2σ) of replicate measurement of the internal standards, was ±0.42‰. Volcanic events in ice cores previously sampled for sulfur isotope studies contained volcanic sulfur concentrations typically 3- to 10-fold greater than background sulfur concentrations (31, 32). Sulfur concentrations during the 17.7ka event were only 1.7 times background (Fig. 4).

In a reinterpretation of the original Byrd core measurements (17), LaViolette (21) proposed an extraterrestrial origin. Helium (He), and especially ^3He, is much higher in extraterrestrial matter than in terrestrial components (57). Approximately 3 kg discrete meltwater samples were collected from the outer ring of the melter head for He concentration and isotope measurements above, within, and below the 17.7ka event. Average ^{3}He concentrations were 4.4e-17 (±2.5e-17) cm^{3} g^{-1} and 3.7e-17 (±2.5e-17) cm^{3} g^{-1} in the five background and four 17.7ka event samples, respectively. Similarly, the ^{3}He/^{4}He ratios were 6.8e-5 (±1.7e-5) in the background samples and 7.3e-5 (±1.9e-5) in the event samples. Interplanetary dust fluxes calculated from these data were in agreement with past measurements (58), indicating no evidence for an extraterrestrial source for the 17.7ka anomaly.

Volcanic Tephra Measurements. Insoluble tephra particles were captured on 10 µm stainless steel filters during continuous analyses for a background section of WD ice with no chemical evidence of volcanic fallout, as well as two sets of filters representing the early and later stages during the extended volcanic period (SI Appendix, Fig. S8). Additional tephra was filtered from larger volume, discrete samples collected as part of targeted replicate coring at WD (SI Appendix – Tephra Sampling and Geochemistry).

Small concentrations of silicate particles were detected for the depth interval corresponding to the early stages of the 17.7ka event (2430–2426 m). No glass shards were found in the background sample or in the sample corresponding to the later stages of the 17.7ka event, consistent with the continuous insoluble particle measurements (SI Appendix, Fig. S1). Most of the particles identified in the sample were fine (~10 µm), and some had cuspate shapes suggestive of volcanic origin. Quantitative geochemical analysis of the particles indicates the presence of volcanic glass with an iron-rich trachytic composition characteristic of West Antarctic volcanism (SI Appendix, Table S1). The two main eruptive source volcanoes in West Antarctica, Mt. Takahe (76^{o} 18.8’S, 112^{o} 4.8’W) and Mt. Berlin (76^{o} 3’S, 136^{o} 0’W), are located 350 km north and 670 km northwest of the WD drilling site, respectively. The composition of tephra erupted from these two volcanoes is similar but can be distinguished by examining the MgO content of the volcanic glass, which is significantly higher in Mt. Takahe eruptions (up to 0.5 wt.%) than in Mt. Berlin eruptions, many of which have undetectable levels of MgO (24, 59).

Break Point Estimates. The BREAKFIT algorithm (60) was used to estimate the timing and uncertainty (1σ) of concentration changes in nssCa, CH_4, and CO_2 (Fig. 2). Intersecting linear trends were fit to nssCa and CH_4 measurements corresponding to 17.0ka to 20.0ka, and CO_2 measurements corresponding to 16.0ka to 20.0ka. Estimated break points for nssCa and CH_4 were 17.882ka (±0.179ka) and 17.759ka (±0.075ka), respectively. Similarly, the break point for CO_2 was 17.612ka (±0.051ka).

Acknowledgements: The U.S. National Science Foundation (NSF) supported this work (0538427, 0839093, 1142166 [J.R.M.]; 1043518 [E.J.B.]; 0538657, 1043421 [J.P.S.], 0538553, 0839066 [J.C.-D.], 0944348, 0944191, 0440817, 0440819, 0230396 [K.C.T.]). We thank the WAIS Divide Science Coordination Office and other support organizations. P.K. and G.K. were funded by PACES-II, with additional support from the Helmholtz Climate Initiative. We acknowledge R. von Glasow for help with snowpack model simulations, and J. Stutz and R. Kreidberg for helpful discussions.

Additional information

Supporting information is available in the online version of the paper.

Competing financial interests

The authors declare no conflicts of interest.

References

1. Hays JD, Imbrie J, & Shackleton NJ (1976) Variations in Earth's orbit - Pacemaker of ice ages. *Science* 194(4270).
2. Cheng H*, et al.* (2009) Ice Age Terminations. *Science* 326(5950):248-252.
3. Landais A*, et al.* (2013) Two-phase change in CO_2, Antarctic temperature and global climate during Termination II. *Nature Geoscience* 6(12):1062-1065.
4. Boex J*, et al.* (2013) Rapid thinning of the late Pleistocene Patagonian Ice Sheet followed migration of the Southern Westerlies. *Sci. Rep.* 3.
5. Moreno P*, et al.* (2015) Radiocarbon chronology of the last glacial maximum and its termination in northwestern Patagonia. *Quaternary Science Reviews* 122:233-249.
6. Putnam A*, et al.* (2013) Warming and glacier recession in the Rakaia valley, Southern Alps of New Zealand, during Heinrich Stadial 1. *Earth and Planetary Science Letters* 382:98-110.
7. Placzek C, Quade J, & Patchett PJ (2006) Geochronology and stratigraphy of late Pleistocene lake cycles on the southern Bolivian Altiplano: Implications for causes of tropical climate change. *Geol. Soc. Am. Bull.* 118(5-6):515-532.
8. Cruz FW*, et al.* (2005) Insolation-driven changes in atmospheric circulation over the past 116,000 years in subtropical Brazil. *Nature* 434(7029):63-66.
9. De Deckker P, Moros M, Perner K, & Jansen E (2012) Influence of the tropics and southern westerlies on glacial interhemispheric asymmetry. *Nat. Geosci.* 5(4):266-269.
10. Martínez-García A*, et al.* (2014) Iron fertilization of the subantarctic ocean during the Last Ice Age. *Science* 343:1347-1350.
11. Lambert F*, et al.* (2008) Dust-climate couplings over the past 800,000 years from the EPICA Dome C ice core. *Nature* 452(7187):616-619.
12. WAIS Divide Project Members (2013) Onset of deglacial warming in West Antarctica driven by local orbital forcing. *Nature* 500(7463):440-444.
13. Cuffey K*, et al.* (2016) Deglacial temperature history of West Antarctica. *Proceedings of the National Academy of Sciences of the United States of America* 113(50):14249-14254.
14. Schmitt J*, et al.* (2012) Carbon isotope constraints on the deglacial CO_2 rise from ice cores. *Science* 336(6082).
15. Marcott SA*, et al.* (2014) Centennial scale changes in the global carbon cycle during the last deglaciation. *Nature* 514:616-619.
16. Voelker C & Koehler P (2013) Responses of ocean circulation and carbon cycle to changes in the position of the Southern Hemisphere westerlies at Last Glacial Maximum. *Paleoceanography* 28(4):726-739.
17. Hammer CU, Clausen HB, & Langway CC (1997) 50,000 years of recorded global volcanism. *Climatic Change* 35(1):1-15.
18. Sigl M*, et al.* (2016) The WAIS Divide deep ice core WD2014 chronology - Part 2: Annual-layer counting (0-31 ka BP). *Clim. Past* 12:769-786.
19. Neumann TA*, et al.* (2008) Holocene accumulation and ice sheet dynamics in central West Antarctica. *Journal of Geophysical Research-Earth Surface* 113(F2):9.

20. Matsumoto A & Hinkley TK (2001) Trace metal suites in Antarctic pre-industrial ice are consistent with emissions from quiescent degassing of volcanoes worldwide. *Earth and Planetary Science Letters* 186(1).
21. LaViolette PA (2005) Solar cycle variations in ice acidity at the end of the last ice age: Possible marker of a climatically significant interstellar dust incursion. *Planetary and Space Science* 53(4).
22. Francis P, Burton MR, & Oppenheimer C (1998) Remote measurements of volcanic gas compositions by solar occultation spectroscopy. *Nature* 396(6711):567-570.
23. Wardell LJ, Kyle PR, & Counce D (2008) Volcanic emissions of metals and halogens from White Island (New Zealand) and Erebus volcano (Antarctica) determined with chemical traps. *Journal of Volcanology and Geothermal Research* 177(3):734-742.
24. Wilch TI, McIntosh WC, & Dunbar NW (1999) Late Quaternary volcanic activity in Marie Byrd Land: Potential Ar-40/Ar-39-dated time horizons in West Antarctic ice and marine cores. *Geological Society of America Bulletin* 111(10).
25. Palais JM, Kyle PR, McIntosh WC, & Seward D (1988) Magmatic and phreatomagmatic volcanic activity at Mt Takahe, West Antarctica, based on tephra layers in the Byrd ice core and field observations at Mt Takahe. *Journal of Volcanology and Geothermal Research* 35(4).
26. Kutterolf S*, et al.* (2013) Combined bromine and chlorine release from large explosive volcanic eruptions: A threat to stratospheric ozone? *Geology* 41(6):707-710.
27. Solomon S*, et al.* (2016) Emergence of healing in the Antarctic ozone layer. *Science* 353(6296):269-274.
28. Ivy D*, et al.* (2017) Observed changes in the Southern Hemispheric circulation in May. *Journal of Climate* 30(2):527-536.
29. Cadoux A, Scaillet B, Bekki S, Oppenheimer C, & Druitt T (2015) Stratospheric ozone destruction by the Bronze-Age Minoan eruption (Santorini Volcano, Greece). *Scientific Reports* 5.
30. Patris N, Delmas RJ, & Jouzel J (2000) Isotopic signatures of sulfur in shallow Antarctic ice cores. *Journal of Geophysical Research-Atmospheres* 105(D6):7071-7078.
31. Baroni M, Thiemens MH, Delmas RJ, & Savarino J (2007) Mass-independent sulfur isotopic compositions in stratospheric volcanic eruptions. *Science* 315(5808):84-87.
32. Savarino J, Romero A, Cole-Dai J, & Thiemens MH (2003) UV induced mass-independent sulfur composition in stratospheric volcanic eruptions. *Geochimica Et Cosmochimica Acta* 67(18):A417-A417.
33. Abbatt JPD*, et al.* (2012) Halogen activation via interactions with environmental ice and snow in the polar lower troposphere and other regions. *Atmos. Chem. Phys.* 12(14):6237-6271.
34. Thomas JL*, et al.* (2011) Modeling chemistry in and above snow at Summit, Greenland - Part 1: Model description and results. *Atmospheric Chemistry and Physics* 11(10):4899-4914.
35. Sigl M*, et al.* (2016) The WAIS Divide deep ice core WD2014 chronology - Part 2: Annual-layer counting (0-31 ka BP). *Clim. Past* 12:769-786.
36. Thompson DWJ*, et al.* (2011) Signatures of the Antarctic ozone hole in Southern Hemisphere surface climate change. *Nature Geoscience* 4(11):741-749.

37. Polvani LM, Waugh DW, Correa GJP, & Son S-W (2011) Stratospheric ozone depletion: The main driver of twentieth-century atmospheric circulation changes in the Southern Hemisphere. *Journal of Climate* 24(3):795-812.
38. Kang SM, Polvani LM, Fyfe JC, & Sigmond M (2011) Impact of polar ozone depletion on subtropical precipitation. *Science* 332(6032):951-954.
39. Waugh DW, Primeau F, DeVries T, & Holzer M (2013) Recent changes in the ventilation of the southern oceans. *Science* 339(6119):568-570.
40. Bitz CM & Polvani LM (2012) Antarctic climate response to stratospheric ozone depletion in a fine resolution ocean climate model. *Geophysical Research Letters* 39.
41. Ferreira D, Marshall J, Bitz C, Solomon S, & Plumb A (2015) Antarctic Ocean and sea ice response to ozone depletion: A two-time-scale problem. *Journal of Climate* 28(3):1206-1226.
42. Solomon A, Polvani L, Smith K, & Abernathey R (2015) The impact of ozone depleting substances on the circulation, temperature, and salinity of the Southern Ocean: An attribution study with CESM1(WACCM). *Geophysical Research Letters* 42(13):5547-5555.
43. Shakun JD*, et al.* (2012) Global warming preceded by increasing carbon dioxide concentrations during the last deglaciation. *Nature* 484:49-54.
44. Baumgartner M*, et al.* (2012) High-resolution interpolar difference of atmospheric methane around the Last Glacial Maximum. *Biogeosciences* 9(10):3961-3977.
45. Gonzalez PM, Polvani L, Seager R, & Correa GP (2013) Stratospheric ozone depletion: A key driver of recent precipitation trends in South Eastern South America. *Climate Dynamics*:1-18.
46. Sugden DE, McCulloch RD, Bory AJM, & Hein AS (2009) Influence of Patagonian glaciers on Antarctic dust deposition during the last glacial period. *Nat. Geosci.* 2(4):281-285.
47. Bauska T*, et al.* (2016) Carbon isotopes characterize rapid changes in atmospheric carbon dioxide during the last deglaciation. *Proceedings of the National Academy of Sciences of the United States of America* 113(13):3465-3470.
48. Mcgee D, Broecker W, & Winckler G (2010) Gustiness: The driver of glacial dustiness? *Quaternary Science Reviews* 29(17-18):2340-2350.
49. Hauck J*, et al.* (2013) Seasonally different carbon flux changes in the Southern Ocean in response to the southern annular mode. *Global Biogeochemical Cycles* 27(4):1236-1245.
50. Son SW*, et al.* (2008) The impact of stratospheric ozone recovery on the Southern Hemisphere westerly jet. *Science* 320(5882):1486-1489.
51. McConnell JR*, et al.* (2014) Antarctic-wide array of high-resolution ice core records reveals pervasive lead pollution began in 1889 and persists today. *Scientific Reports* 4(5848):1-5.
52. Sigl M*, et al.* (2015) Timing and climate forcing of volcanic eruptions for the past 2,500 years. *Nature* 523(7562):543-549.
53. Maselli OJ*, et al.* (2017) Sea ice and pollution-modulated changes in Greenland ice core methanesulfonate and bromine. *Climate of the Past* 13:39-59.
54. McConnell JR & Edwards R (2008) Coal burning leaves toxic heavy metal legacy in the Arctic. *Proceedings of the National Academy of Sciences of the United States of America* 105(34):12140-12144.

55. Baggenstos D (2015) Taylor Glacier as an archive of ancient ice for large-volume samples: Chronology, gases, dust, and climate. Ph.D. (University of California, San Diego).
56. Paris G, Sessions AL, Subhas AV, & Adkins JF (2013) MC-ICP-MS measurement of delta S-34 and Delta S-33 in small amounts of dissolved sulfate. *Chemical Geology* 345:50-61.
57. Farley KA & Mukhopadhyay S (2001) An extraterrestrial impact at the Permian-Triassic boundary? *Science* 293(5539):2343-+.
58. Winckler G & Fischer H (2006) 30,000 years of cosmic dust in Antarctic ice. *Science* 313(5786).
59. Dunbar NW, McIntosh WC, & Esser RP (2008) Physical setting and tephrochronology of the summit caldera ice record at Mount Moulton, West Antarctica. *Geological Society of America Bulletin* 120(7-8).
60. Mudelsee M (2009) Break function regression. *European Physical Journal-Special Topics* 174:49-63.
61. Rhodes RH, *et al.* (2015) Enhanced tropical methane production in response to iceberg discharge in the North Atlantic. *Science* 348(6238):1016-1019.

Figure Legends

Fig. 1 Changes in climate indicators during the last glacial termination relative to the 17.7ka glaciochemical anomaly. Shading shows the ~192-year glaciochemical anomaly. (**a**) Annually integrated (12) 65°S insolation and (**b**) WD $\delta^{18}O$ (12); (**c**) WD CO_2 (15) and (**d**) Taylor Glacier $\delta^{13}C$ of CO_2 synchronized to the WD CO_2 record (47); (**e**) WD CH_4 (61) and (**f**) WD mineral acidity, SH dust proxies, (**g**) WD nssCa, and (**h**) EPICA Dome C (EDC) (11) in ice cores, with the latter synchronized to WD using volcanic events; (**i**) Fe measured in a South Australian ocean sediment core (9); (**j**) the surface UV indicator Br in the WD core; (**k**) Botuvera speleothem $\delta^{18}O$ that is a proxy for summertime precipitation in southeastern Brazil (8).

Fig. 2 Selected high-resolution elemental and gas phase measurements through the ~192-year glaciochemical anomaly in the WD ice core at 17.7ka (gray shading) showing nine distinct pulses. Acidity, low-boiling-point heavy metals (e.g., Bi), and halogens (e.g., Cl) other than Br (Fig. 1) were highly elevated throughout the anomaly (SI Appendix, Fig. S1), with REE (e.g., Ce) enhanced only during the first ~120 years. SH dust indicators (e.g., nssCa) were elevated only slightly and slowly increasing GHG [CH_4 (61), CO_2 (15)] concentrations accelerated during the event (Fig. 1). Measurements in the Byrd core are similar (SI Appendix, Fig. S2). Calculated break points (1σ uncertainty) suggest that long-term changes in nssCa, CH_4, and CO_2 concentrations in the WD core began during the 17.7ka anomaly (Materials and Methods).

Fig. 3 Spatial extent of the glaciochemical anomaly. Evidence of the ~192-year anomaly has been found >2800 km from Mt. Takahe in ice core (circles) chemical records (SI Appendix, Fig. S3) as well as radar surveys from much of West Antarctica. Also shown are area volcanoes (triangles). Sep/Oct horizontal wind vectors at 600 hPa based on 1981 to 2010 National Centers for Environmental Prediction (NCEP) reanalysis fields show transport patterns consistent with observations.

Fig. 4 Sulfur isotope anomalies indicate changes in UV radiation during the 17.7ka event. Despite relatively modest increases in sulfur concentration in both the WD and Byrd records, volcanic sulfur emissions led to decreased $\delta^{34}S$, while increased UV radiation resulted in anomalous $\Delta^{33}S$. Uncertainties are 2σ.

Fig. 5 Observed and modeled SH precipitation anomalies linked to modern stratospheric ozone depletion. Shown are observed and modeled zonal mean austral summer (DJF) net precipitation changes between 1979 and 2000 (38). Changes represent a ~10% increase between 15° and 35°S relative to the climatology (38). Simulated LGM responses to stratospheric ozone depletion are qualitatively similar (SI Appendix – AOGCM Simulations). Approximate latitude ranges for SH aridity and glacial outwash dust sources as well as wetlands during the LGM are indicated. Sharp changes in SH climate proxies occur exactly at this time (4, 6, 7, 10, 11, 14) (Fig. 1).

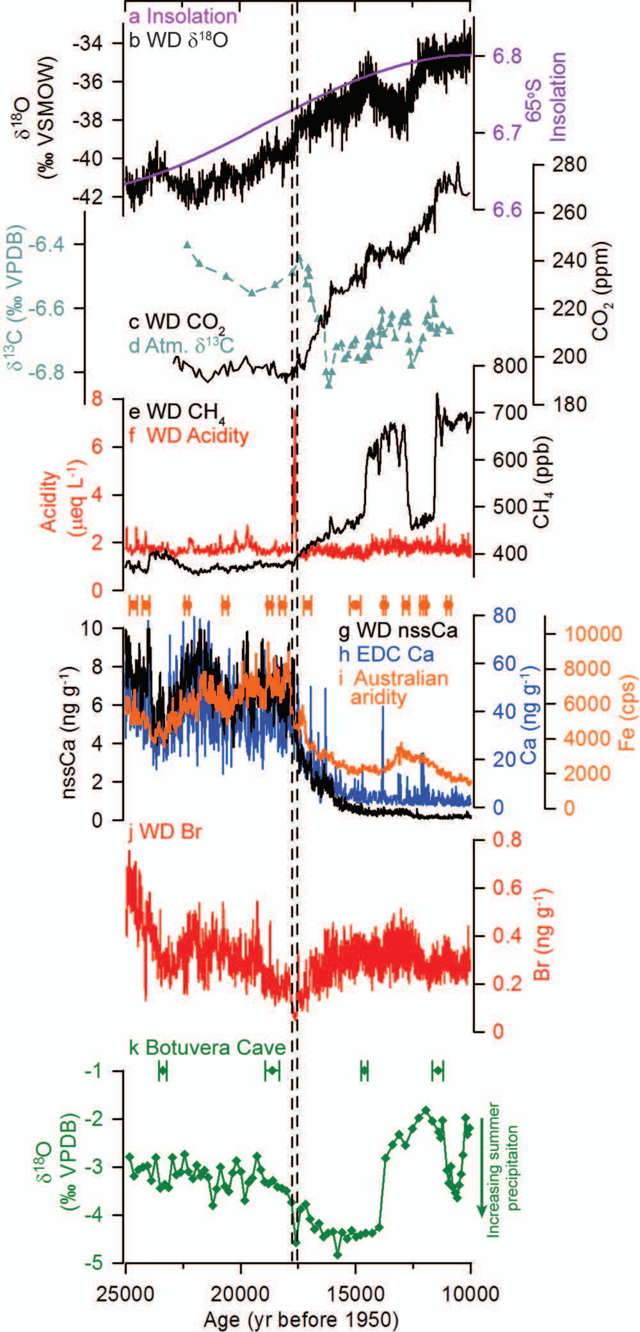

a Insolation
b WD δ18O
δ18O (‰ VSMOW)
65°S Insolation
c WD CO2
d Atm. δ13C
δ13C (‰ VPDB)
CO2 (ppm)
e WD CH4
f WD Acidity
Acidity (µeq L-1)
CH4 (ppb)
g WD nssCa
h EDC Ca
i Australian aridity
nssCa (ng g-1)
Ca (ng g-1)
Fe (cps)
j WD Br
Br (ng g-1)
k Botuvera Cave
δ18O (‰ VPDB)
Increasing summer precipitaiton
Age (yr before 1950)

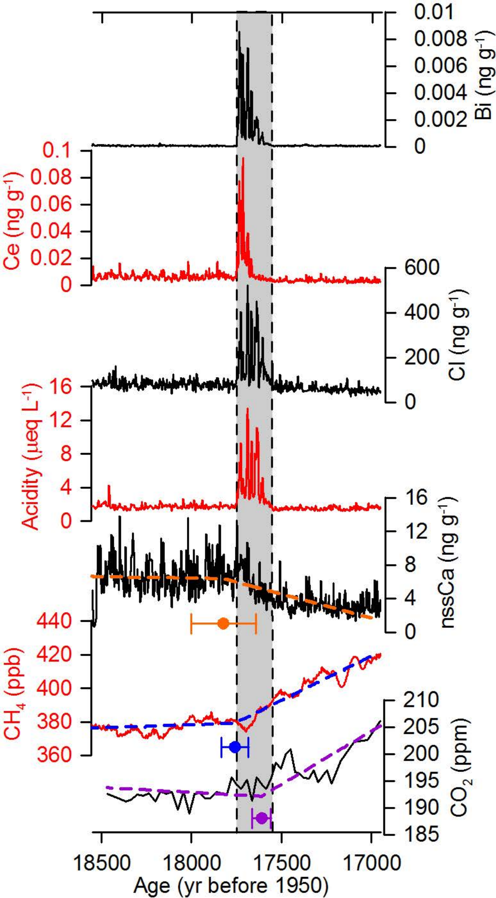

Bi (ng g-1)
Ce (ng g-1)
Cl (ng g-1)
Acidity (μeq L-1)
nssCa (ng g-1)
CH4 (ppb)
CO2 (ppm)
Age (yr before 1950)

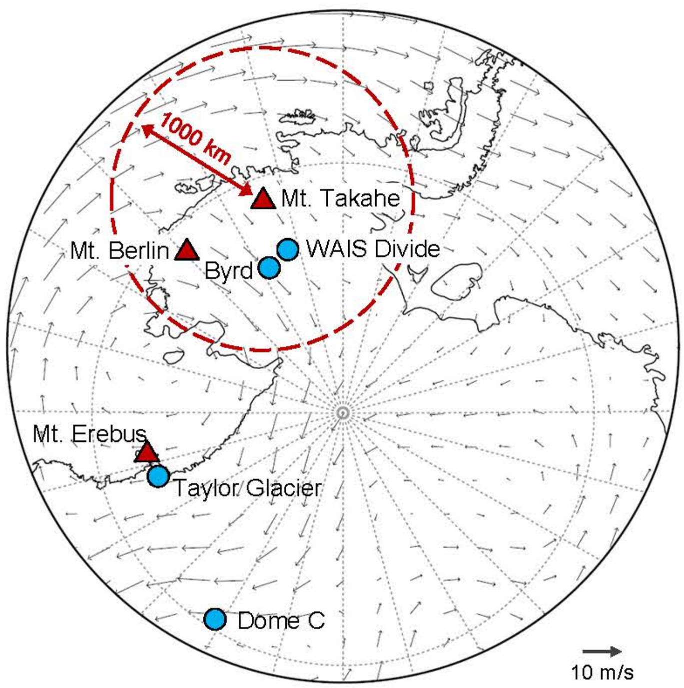
1000 km
Mt. Takahe
Mt. Berlin
WAIS Divide
Byrd
Mt. Erebus
Taylor Glacier
Dome C
10 m/s

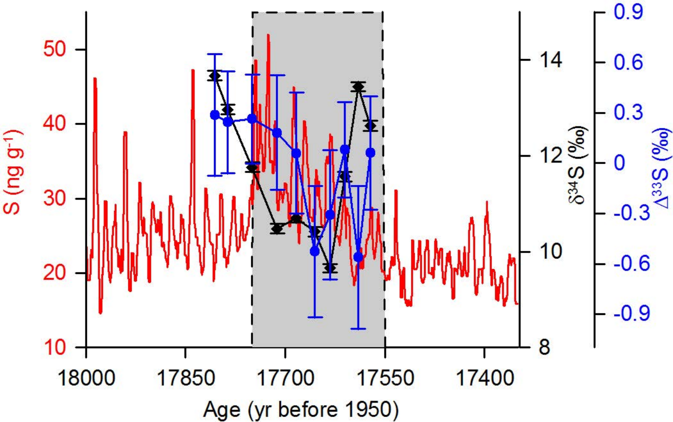
S (ng g-1)
50
40
30
20
10
18000
17850
17700
17550
17400
Age (yr before 1950)
14
12
10
8
δ34S (‰)
0.9
0.6
0.3
0
-0.3
-0.6
-0.9
Δ33S (‰)

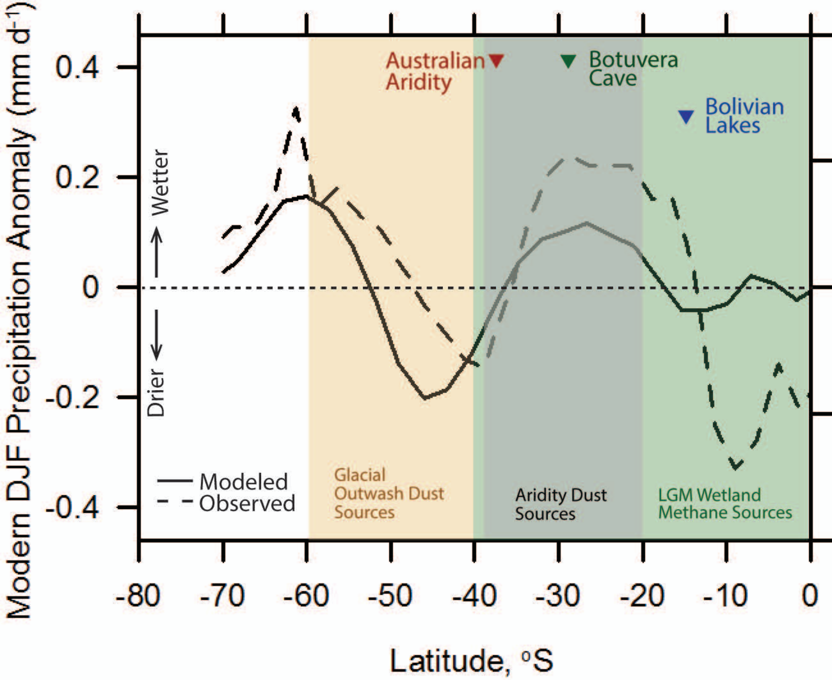

Modern DJF Precipitation Anomaly (mm d-1)
0.4
0.2
0
-0.2
-0.4
Wetter
Drier
Australian Aridity
Botuvera Cave
Bolivian Lakes
Modeled
Observed
Glacial Outwash Dust Sources
Aridity Dust Sources
LGM Wetland Methane Sources
-80
-70
-60
-50
-40
-30
-20
-10
0
Latitude, °S